

Structural and Theoretical Analysis of M–H- -H–M and M–H- -H–C Intermolecular Interactions

Dario Braga,^{*,†} Piero De Leonardis,[†] Fabrizia Grepioni,[†] Emilio Tedesco,[†] and Maria José Calhorda^{*,‡}

Dipartimento di Chimica G. Ciamician, Università di Bologna, Via Selmi 2, 40126 Bologna, Italy, and ITQB, Quinta do Marquês, EAN, Apart. 127, 2780 Oeiras, and Dep. Química e Bioquímica, Faculdade de Ciências, Campo Grande, 1700 Lisboa, Portugal

Received August 8, 1997

The relationship between molecular and crystal structures of organometallic complexes showing intermolecular interactions of the M–H- -H–M and M–H- -H–C type has been investigated by a combined use of extended Hückel and DFT calculations, and crystal packing analysis. Molecular and crystal structures determined by neutron and/or X-ray diffraction experiments of coordination complexes and clusters showing intermolecular M–H- -H–M and M–H- -H–C interactions below 2.6 Å have been retrieved from the Cambridge Structural Database. Molecular orbital analysis has been carried out by means of extended Hückel and DFT calculations on selected compounds. For the HMn(CO)₅ dimer, where the interaction is of the M–H- -H–M type, the system is reminiscent of a bound hydrogen molecule where the H–H bond has been greatly weakened. A very small binding energy of ca. 5 kJ mol⁻¹ has been determined using DFT calculations. This simple interpretation does not hold in the cases of M–H- -H–C short contacts, which are more appropriately described as arising from a special type of hydrogen bond associated with opposite charges on the two hydrogen atoms.

Introduction

Hydrogen bonding interactions formed by transition metal organometallic complexes are being extensively investigated since the discovery of several hydrogen bonding donor and acceptor groups which have no counterpart in organic systems.¹

The transition metal–hydride (M–H) system, for example, has been shown to have an amphoteric behavior. When the hydrogen atom is bound in edge- or face-bridging fashion in polynuclear electron-rich transition metal clusters, the M–H system behaves as an hydrogen bonding donor group.² It is comparable in strength to the C(sp)–H and C(sp²)–H systems and, as these donors, interacts with organometallic acceptors such as the CO ligand in its various bonding modes.³ On the other hand, the M–H system in mononuclear complexes has also been recently shown to be able to establish intramolecular and intermolecular interactions of the M–H- -H–X type (X = C, N, O, S). That these latter interactions can be weakly attractive in nature has been recently demonstrated by spectroscopic,⁴ and diffraction⁵ experiments and discussed in theoretical studies.⁶

M–H- -OC and M–H- -H–X interactions demonstrate the duality of the M–H system with regard to its participation in

hydrogen bonding interactions. Clearly, the assessment of the acid–base behavior of metal atoms as well as of the M–H system and its dependence on coordination mode, oxidation state, and nature of the other ligands is complicated but is also a challenging and fascinating problem. Some useful steps forward have been recently made.⁷

Recently we addressed the problem of the existence of short H- -H intramolecular contacts in transition metal organometallic hydride complexes and found out that attractive interactions between a hydride and a hydrogen atom attached to an electronegative atom such as O or N coexist with situations where those atoms are forced into close vicinity by extrinsic factors.⁸

In this work, we have extended the investigation of H- -H interactions by searching the Cambridge Structural Database⁹ for the occurrence of intermolecular interactions of the

* Corresponding authors. E-mail: dlab@ciam.unibo.it and mjc@itqb.unl.pt.

† Università di Bologna.

‡ ITQB and Universidade de Lisboa.

- (1) (a) Braga, D.; Grepioni, F. *Chem. Commun.* **1996**, 571. (b) Braga, D.; Grepioni, F. *Acc. Chem. Res.* **1997**, *30*, 81. (c) Brammer, L.; Zhao, D.; Ladipo, F. T.; Braddock-Wilking, J. *Acta Crystallogr. Sect. B* **1995**, *B51*, 632. (d) Crabtree, R. H.; Siegbahn, P. E.; Eisenstein, O.; Rheingold, A. L.; Koetzle, T. F. *Acc. Chem. Res.* **1996**, *29*, 348.
- (2) Braga, D.; Grepioni, F.; Tedesco, E.; Desiraju, G. R.; Biradha, K. *Organometallics* **1996**, *15*, 2692.
- (3) Braga, D.; Biradha, K.; Grepioni, F.; Pedireddi, V. R.; Desiraju, G. R. *J. Am. Chem. Soc.* **1995**, *117*, 3156.

- (4) (a) Shubina, E. S.; Belkova, N. V.; Krylov, A. N.; Vorontsov, E. V.; Epstein, L. M.; Gusev, D. G.; Niedermann, M.; Berke, H. *J. Am. Chem. Soc.* **1996**, *118*, 1105. (b) Belkova, N. V.; Shubina, E. S.; Ionidis, A. V.; Epstein, L. M.; Jacobsen, H.; Messmer, A.; Berke, H. *Inorg. Chem.* **1997**, *36*, 1522. (c) Peris, E.; Lee, J. C., Jr.; Rambo, J. R.; Eisenstein, O.; Crabtree, R. H. *J. Am. Chem. Soc.* **1995**, *117*, 3485. (d) Fairhurst, S. A.; Henderson, R. A.; Hughes, D. L.; Ibrahim, S. K.; Pickett, C. J. *J. Chem. Soc., Chem. Commun.* **1995**, 1569. (e) Lough, A. J.; Park, S.; Ramachandran, R.; Morris, R. H. *J. Am. Chem. Soc.* **1994**, *116*, 8356. (f) Aime, S.; Gobetto, R.; Valls, E. *Organometallics* **1997**, *16*, 5140.
- (5) Wessel, J.; Lee, J. C., Jr.; Peris, E.; Yap, G. P. A.; Fortin, J. B.; Ricci, J. S.; Sini, G.; Albinati, A.; Koetzle, T. F.; Eisenstein, O.; Rheingold, A. L.; Crabtree, R. H. *Angew. Chem., Int. Ed. Engl.* **1995**, *34*, 2507.
- (6) Liu, Q.; Hoffmann, R. *J. Am. Chem. Soc.* **1995**, *117*, 10108.
- (7) Braga, D.; Grepioni, F.; Tedesco, E.; Birhadha, K.; Desiraju, G. R. *Organometallics* **1997**, *16*, 1846.
- (8) Braga, D.; Grepioni, F.; Tedesco, E.; Calhorda, M. J.; Lopes, P. E. M. *New J. Chem.*, submitted.
- (9) Allen, F. H.; Davies, J. E.; Galloy, J. J.; Johnson, O.; Kennard, O.; Macrae, C. F.; Watson, D. G. *J. Chem. Inf. Comput. Sci.* **1991**, *31*, 204.

M–H...H–M and M–H...H–C type (M = transition metal) between molecules or ions in the solid state. This work attempts to understand the electronic nature and origin of these interactions by means of crystal packing analysis¹⁰ and theoretical methods, namely extended Hückel¹¹ and DFT.¹²

Results and Discussion

The structures to analyze have been selected from those retrieved from the Cambridge Structural Database⁹ (see Experimental Section). The selection criterion was based on H...H distances obtained after normalization of the X–H bond lengths to neutron-derived values in the case of hydrogen atoms bound to main group elements (X = C, N, O, S). M–H distances were kept at the observed values. The CSD search yielded five structures of metal hydride complexes showing M–H...H–M and 288 structures showing M–H...H–C contact distances less than 2.6 Å (see Experimental Section). CSD REFCODES will initially accompany chemical formulas and will then be used throughout this paper to refer to the structures. Complexes chosen for this analysis are listed in Table 1 together with the relevant structural parameters and references to the original structural papers. Geometrical questions for the two CSD searches are available as Supporting Information.

Each structure listed in Table 1 has been analyzed in terms of intermolecular hydrogen bonding interactions both of conventional and of the H...H type. The paper is organized in two distinct sections dealing with M–H...H–M and M–H...H–C interactions. Representative cases have been subjected to molecular orbital calculations.

Intermolecular Interactions of the M–H...H–M Type.

The complex HMn(CO)₅, FOKCEN02, was one of the first carbonyl hydrides to be structurally characterized by X-ray and neutron diffraction.¹³ In 1968, when the neutron diffraction study was published, the authors were already aware of the presence of short H...H contacts between pairs of molecules in the crystal. This peculiar intermolecular contact between hydride ligands attracted our interest and prompted our investigation.

HMn(CO)₅ is found in the solid state in two polymorphic forms, both monoclinic, namely α -HMn(CO)₅ and β -HMn(CO)₅. In the former, the hydride position was not localized even by a low-temperature X-ray study, whereas in the second polymorph a neutron determination was carried out for a precise measure, giving a H...H intermolecular distance of 2.292 Å. An accurate examination of the packing of both phases resulted in very small differences, the main packing motif being preserved. We shall refer hereafter to the β form, of which the packing arrangement is illustrated in Figure 1.

The intermolecular dimers present in the β form of HMn(CO)₅ are appealing for an intermolecular molecular orbital analysis. The structure of the molecule has also been determined by electron diffraction¹⁴ and a distortion of the four equatorial carbonyl groups toward the hydride is observed in the gas phase as well as in the solid state. This distortion has been studied

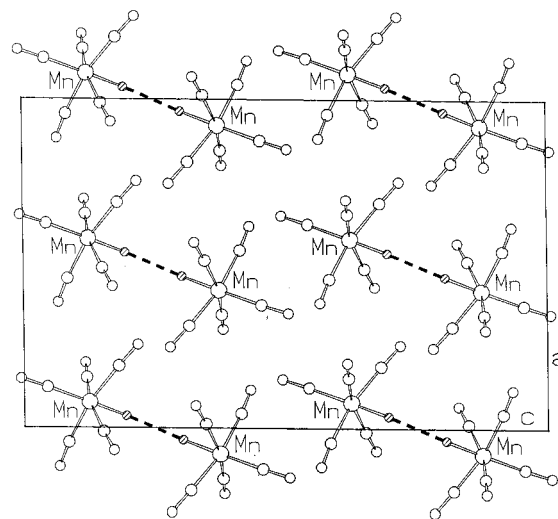


Figure 1. Molecular organization in crystalline HMn(CO)₅, FOKCEN02. Note how the molecules form “dimers” via H...H contact pairs.

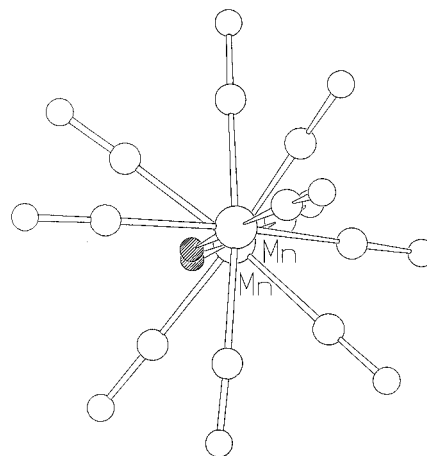


Figure 2. Two staggered HMn(CO)₅ units in the crystal structure face each other at an Mn–H...H angle of 155.8°.

by EH calculations and traced to several factors, including a better overlap between π^* of equatorial carbonyl orbitals and manganese orbitals.¹⁵ DFT studies of the hydride and several other related Mn(CO)₅ derivatives are also reported¹⁶ and in a general way lead to a good agreement between experimental and observed structures. The problem of the formation of the dimer in the solid state has not yet, to our knowledge, been addressed.

The two HMn(CO)₅ units face each other at an angle of 155.8° (formed between the O–C–Mn–H axes) and are staggered so that only one mirror plane is present (Figure 2) in the dimer.

If these two units are allowed to approach so that the two hydrides get closer, an energy minimum is observed in the extended Hückel calculations, which depends on the approaching geometry. The details of calculations are reported in the experimental part. For a linear approach with either eclipsed or staggered orientations of the monomers, for instance, the binding energy is -0.07 eV (note that 1 eV = 96.48 kJ mol⁻¹) for an H...H distance of 1.6 Å (overlap population, OP, is 0.089). The binding energy, BE, is the difference between the energy of the dimer and the sum of the energies of two

- (10) (a) Braga, D.; Grepioni, F.; Wadehohl, H.; Gebert, S.; Calhorda, M. J.; Veiros, L. F. *Organometallics* **1995**, *14*, 24. (b) Braga, D.; Grepioni, F.; Calhorda, M. J.; Veiros, L. *Organometallics* **1995**, *14*, 5350.
 (11) (a) Hoffmann, R. *J. Chem. Phys.* **1963**, *39*, 1397. (b) Hoffmann, R.; Lipscomb, W. N. *J. Chem. Phys.* **1962**, *36*, 2179; 3489.
 (12) *Amsterdam Density Functional (ADF) Program*, Release 2.01; Vrije Universiteit: Amsterdam, The Netherlands, 1995.
 (13) La Placa, S. J.; Hamilton, W. C.; Ibers, J. A.; Davison, A. *Inorg. Chem.* **1969**, *8*, 1928.
 (14) McNeill, E.; Scholer, F. R. *J. Am. Chem. Soc.* **1977**, *99*, 6243.

- (15) Jackson, S. A.; Eisenstein, O.; Martin, M. D.; Albeniz, A. C.; Crabtree, R. H. *Organometallics* **1991**, *10*, 3061.
 (16) Folga, E.; Ziegler, T. *J. Am. Chem. Soc.* **1993**, *115*, 5169.

Table 1. Compound Formulas, REFCODES (in Alphabetical Order), and Relevant Geometrical Parameters for M-H...H Intermolecular Interactions for Transition Metal Complexes Showing M-H...H-M and/or M-H...H-C Distances Shorter than 2.3 Å; C-H...O Bonds (<2.6 Å) Are Also Reported

compound REFCODE ^a	M-H (Å)	H...H (Å)		X-H...Y Inter Å		X-H...Y (deg)	ref
[(Ph ₃ P) ₂ N][H ₂ W ₂ (CO) ₈] BIKBEC01 ^b	1.920(3)	H(1)...H(15)	2.150	C(7)-H(5)...O(4)	2.477	146.6	28
	1.933(2)			C(13)-H(10)...O(2)	2.478	159.8	
				C(22)-H(16)...O(2)	2.562	161.6	
				C(25)-H(18)...O(3)	2.565	138.4	
				C(26)-H(19)...O(3)	2.514	137.3	
				C(27)-H(20)...O(4)	2.489	164.7	
				C(31)-H(23)...O(1)	2.495	116.7	
				C(36)-H(27)...O(4)	2.529	130.5	
				C(1)-H(1)...O(12)	2.516	148.7	
				C(4)-H(4)...O(12)	2.515	147.8	
(η ⁵ -C ₅ H ₅) ₂ TaH(CO) BISZIM	1.79(6)	H(11)...H(3)	1.957	C(5)-H(5)...O(12)	2.463	156.0	29
				C(9)-H(9)...O(12)	2.400	151.5	
				C(12)-H(12)...O(2)	2.382	149.8	
				C(14)-H(14)...O(1)	2.572	163.9	
[(η ⁵ -C ₅ H ₅) ₂ MoH(CO)] [(η ⁵ -C ₅ H ₅) ₂ Mo(CO) ₃] CPCBMO01	1.87(7)	H(1)...H(1)	2.234	C(6)-H(6)...O(2)	2.393	138.5	17
				C(9)-H(9)...O(1)	2.476	127.4	
				C(12)-H(12)...O(2)	2.382	149.8	
				C(16)-H(16)...O(1)	2.490	140.2	
				C(18)-H(18)...O(2)	2.434	161.3	
				C(11)-H(2)...O(9)	2.529	139.4	
(μ-H) ₂ Os ₅ (μ ₃ -CH ₂)(CO) ₁₀ DCHMOS01 ^b	1.834(11)	H(1)...H(4)	2.085	(Intra)			30
	1.808(10)						
HMn(CO) ₅ FOKCEN02 ^b	1.601(16)	H(1)...H(1)	2.292				13
ReH(CO) ₂ (PMe ₃) ₃ HAKCUR	1.99(8)	H(56)...H(16)	1.839	C(12)-H(22)...O(4)	2.514	159.9	31
ReH ₃ (CO)(PMe ₃) ₃ HAKDEC	1.73(5)	H(1)...H(43)	1.890	C(3)-H(7)...O(1)	2.437	163.3	31
				C(4)-H(10)...O(1)	2.566	162.1	
				C(6)-H(17)...O(2)	2.498	156.4	
<i>trans</i> -[PtH(PhHNNC ₃ H ₆)(PPh ₃) ₂][BF ₄][C ₆ H ₆] HAPZPT10	1.65 ^c	H(8)...H(45)	2.092	N(2)-H(7)...F(1)	2.043	144.9	32
				C(6)-H(10)...F(4)	2.369	132.9	
				C(12)-H(15)...F(2)	2.386	134.1	
				C(32)-H(32)...F(4)	2.550	121.1	
				C(37)-H(36)...F(3)	2.333	151.2	
(η ⁵ -C ₅ Me ₄ Et)(η ⁵ -C ₅ H ₅)ReH JASRAW	1.68(7)	H(1)...H(2)	1.773				33
<i>trans</i> -RuH(Cl)L, L = <i>syn</i> -Me ₄ [14]aneS ₄ KEGCEE	1.68(8)	H(1)...H(4)	2.009	C(1)-H(3)...Cl(1)	2.629	127.0	34
				C(12)-H(22)...Cl(1)	2.668	160.3	
				C(12)-H(23)...S(1)	2.703	161.2	
				C(14)-H(27)...Cl(1)	2.690	170.1	
<i>mer</i> -[(Me ₃ P) ₃ IrH(C ₅ H ₄ N)][Cl] LANMES	1.69 ^d	H(1)...H(16)	2.106				26
(η ⁵ -C ₅ H ₅) ₂ TaH ₃ TACPTH ^b	1.769(8)	H(11)...H(10)	2.002				35
		H(13)...H(7)	2.093				
H ₄ Os(PPhMe ₂) ₃ THMPOS01 ^b	1.648(3)	H(2)...H(31)	2.062				36
[H ₅ Os(PPhMe ₂) ₃][BF ₄] YELZOE ^b	1.64(2)	H(2)...H(6)	2.114	C(5)-H(13)...F(3)	2.469	138.9	37
				C(10)-H(22)...F(2)	2.225	148.5	
				C(14)-H(25)...F(3)	2.507	148.4	
				C(18)-H(31)...F(1)	2.375	144.0	
				C(18)-H(33)...F(3)	2.282	162.2	
				C(22)-H(36)...F(3)	2.291	163.4	
[(η ⁵ -C ₅ H ₅) ₂ Zr(μ-H)(OSO ₂ CF ₃) ₂ ·0.5THF YUSSOU	1.831(9)	H(1)...H(1)	2.122	C(2)-H(3)...O(2)	2.492	126.6	22
				C(9)-H(10)...O(1)	2.442	152.5	

^a Atom labeling is that present in CSD. ^b Neutron study. ^c Based on normalized C-H, N-H, and O-H distances. ^d M-H distance not reported in the original paper.

monomers. On the other hand, if the monomers approach along the observed direction (angle of 155.8°) with staggered orientation, the minimum is less pronounced (binding energy -0.01 eV) but the experimental H...H distance is in much better agreement (2.28 Å, OP 0.029). The smaller overlap population reflects the longer distance, but it is still positive. This same approach keeping the eclipsed arrangement of the carbonyls is repulsive, as the carbonyl groups belonging to adjacent molecules come into close contact. The observed staggered conformation is therefore preferred for steric reasons.

Another bimolecular approach which is very interesting to consider is the one implying an interaction between CO and the M-H bond, Mn-C-O...H-Mn, as such situations are commonly found in other structures, namely [(η⁵-C₅H₅)₂MoH-

(CO)][(η⁵-C₅H₅)Mo(CO)₃], CPCBMO01 (see below), and (η⁵-C₅H₅)₂TaH(CO), BISZIM, to mention only the set of structures under study.^{17,18} We tried to model this hypothetical dimer, but as the two units got closer, a strong repulsion developed irrespective of the geometry of approach (linear, bent, eclipsed, or staggered). Therefore, on electronic grounds we found a reason for the experimentally observed H...H bound structure, rather than for a H...O-C one.

Although the dimer contains staggered HMn(CO)₅ units, the

- (17) Antsyshkina, A. S.; Dikareva, L. M.; Porai-Koshits, M. A.; Ostrikova, V. N.; Skripkin, Yu. V.; Volkov, O. G.; Pasynskii, A. A.; Kalinnikov, V. T. *Koord. Khim.* **1985**, *11*, 82.
(18) Marsella, J. A.; Huffman, J. C.; Caulton, K. G.; Longato, B.; Norton, J. R. *J. Am. Chem. Soc.* **1982**, *104*, 6360.

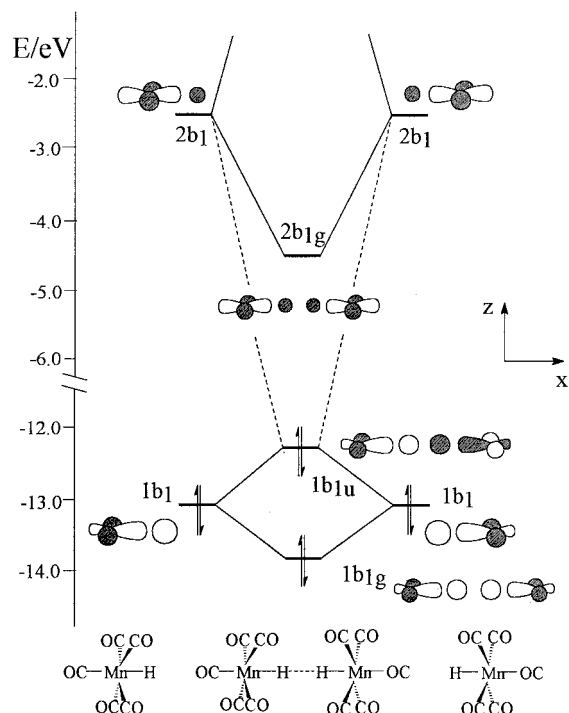


Figure 3. Interaction diagram between two $\text{HMn}(\text{CO})_5$ monomers.

EH analysis¹⁹ will be based on the linear, eclipsed approach, to take advantage of the higher C_{4v} symmetry. The situation is otherwise comparable. The interaction between the two monomers is depicted schematically in Figure 3. Indeed the Mn–H bond is formed by σ -donation from the hydrogen 1s orbital to a σ -acceptor orbital of the C_{4v} ML_5 fragment,^{15,19} and for simplicity only the two molecular orbitals, $1b_1$ and $2b_1$, resulting from such interaction are drawn. As expected, only the bonding, low-energy counterpart $1b_1$ is occupied in the monomer.

When the monomers approach, there is a strong four-electron destabilizing interaction between the two filled $1b_1$ orbitals. However, the empty set of antibonding Mn–H $2b_1$ orbitals mixes in a bonding way¹⁹ into b_{1u} so that the H–H antibonding character is partially relieved, making the global interaction an attractive one (the H–H overlap population is 0.134). This bonding pattern is similar to the one found in other weak interactions, such as Au(I)–Au(I) short contacts.²⁰

Another suggestion of how to look at the bonding in this dimeric species is to relate it with the well-known hydrogenation of $\text{Mn}_2(\text{CO})_{10}$, which gives rise to $\text{HMn}(\text{CO})_5$. The solid-state structure may be considered as a point along the hydrogenation reaction pathway taking decacarbonyldimanganese into the manganese hydride. Ziegler and co-workers studied the hydrogenation reaction using DFT calculations and found an activation barrier of 40 kJ mol⁻¹ in good agreement with the experimental value of 34.6 ± 1 kJ mol⁻¹.¹⁶ The photodissociation of $\text{Mn}_2(\text{CO})_{10}$ was also studied by means of DFT calculations and may also be related to the problem under study.²¹

To address this problem, we considered the $\text{Mn}_2(\text{CO})_{10}$ dimer in its more symmetric eclipsed conformation and approached

- (19) Albright, T.; Burdett, J. K.; Whangbo, M.-H. *Orbital Interactions in Chemistry*; John Wiley & Sons: New York, 1985.
 (20) (a) Jiang, Y.; Alvarez, S.; Hoffmann, R. *Inorg. Chem.* **1985**, *24*, 749.
 (b) Veiros, L. F.; Calhorda, M. J. *J. Organomet. Chem.* **1994**, *478*, 37.
 (21) Rosa, A.; Ricciardi, G.; Baerends, E. J.; Stufkens, D. *J. Inorg. Chem.* **1996**, *35*, 2886.

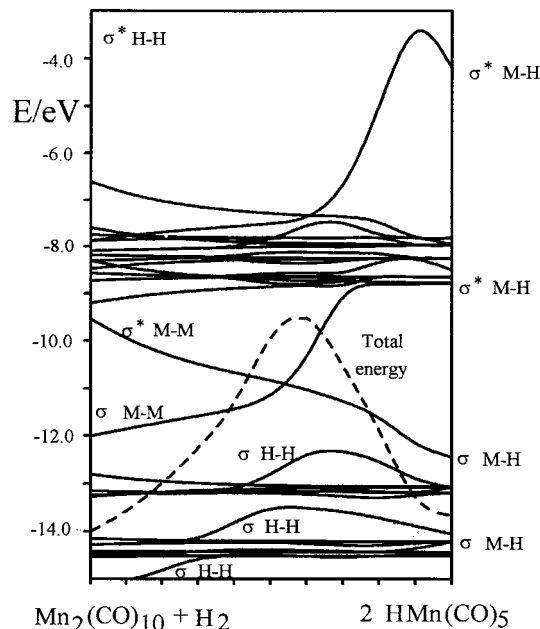
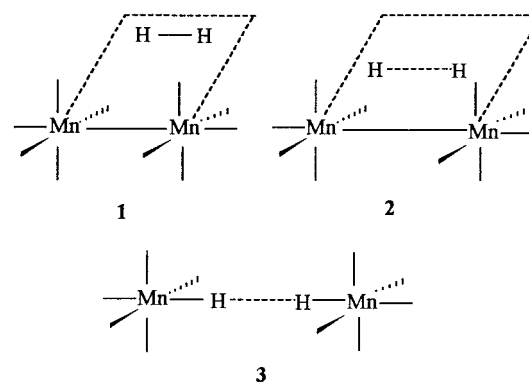


Figure 4. Walsh diagram for the insertion of one H_2 molecule into the Mn–Mn bond of $\text{Mn}_2(\text{CO})_{10}$.

Chart 1



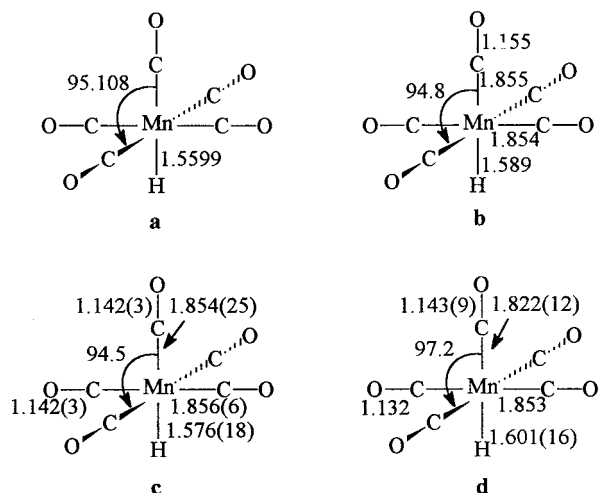
one H_2 molecule. To minimize steric constraints, the hydrogen molecule was allowed to insert in the Mn–Mn bond coming in a plane bisecting the planes containing the carbonyl groups, as sketched in Chart 1. There is a mirror plane while insertion takes place.

The Walsh diagram shows this to be a symmetry-forbidden reaction, as indicated by the crossing of the HOMO (σ Mn–Mn) and the LUMO (σ^* Mn–Mn), which have different symmetry, Figure 4.

The total energy is shown by the dashed line (same scale as the molecular orbitals), and the activation energy for the reaction is estimated as ca. 4.5 eV, which is much higher than the value calculated by Ziegler and co-workers¹⁶ and can only be taken as indicative. The reaction is forbidden, as the HOMO on the left side (the σ Mn–Mn level) is destabilized with the breaking of the Mn–Mn bond, ending as a high-energy empty orbital. Conversely, the LUMO, the σ^* Mn–Mn level is stabilized for the same reason. The high activation barrier can be assigned both to breaking the Mn–Mn bond and strongly weakening the H–H bond (note the destabilization of the σ H–H level), while the stabilization seen in the last steps is due to the formation of the two new Mn–H bonds.

While the real reaction cannot be exactly compared, as it takes place in solution and a monomeric product is formed, this

Chart 2



interpretation might be envisaged as a first approach to study a solid-state reaction.

The $\text{HMn}(\text{CO})_5$ dimer was also studied using DFT calculations (ADF program)¹² in order to determine the bonding energy between the two units in a more reliable way. The geometry of the monomer was first optimized, keeping C_{4v} symmetry and allowing only the Mn-H distance and the H-Mn-C_{eq} angle to vary. All variables could be optimized for the monomer, but it would be difficult to proceed similarly for the dimer, as the size doubles and symmetry is greatly reduced, and it is important to keep the same conditions. Nonlocal corrections were added during the optimization procedure (see Experimental Section for further details). The results of our geometry optimization are shown in Chart 2 a with those of Folga and Ziegler,¹⁶ who used the same method (Chart 2b), and the experimental data, both in the gas phase (Chart 2c) and in the crystal (Chart 2d).

The geometrical agreement between the geometry we obtained and the gas-phase one is not as good as the one of Folga and Ziegler,¹⁶ probably because a complete optimization was not attempted. On the other hand, we want to study the solid for which the distances and angles are also different. Besides the intramolecular ones shown in Chart 2d, the H...H distance is 2.291 Å, the Mn...Mn distance is 5.212 Å, and the H...H-Mn angle is 155.8°, the two hydrides and the two manganese atoms being coplanar. The two units are staggered as already mentioned, so that the final symmetry is only C_s . The potential energy surface for the approach of the two $\text{HMn}(\text{CO})_5$ units is very flat. In these calculations, only the approach geometry was allowed to change, the monomer being kept fixed. For an eclipsed approach, the binding energy, taken as the difference between the energy of the dimer and twice the energy of the monomer, was found to be -0.003 eV, meaning that there is a weak attraction. The equilibrium H...H distance was 2.008, Mn-H was 1.559 Å, and the angle between the two Mn-H axes was 147°.

For the staggered geometry, the results are not so rewarding, as the best energy was found for a H...H distance of 1.68 Å and an angle between the two Mn-H axes of 167.4°. It should be taken into account that the potential energy surface is very flat and that this may not be the global maximum. However, the binding energy still corresponds to a stabilizing interaction and is essentially the same as for the eclipsed conformer.

In conclusion, both our approaches indicate a weak tendency of $\text{Mn}(\text{CO})_5\text{H}$ to form a dimer, as observed in the solid-state structure.

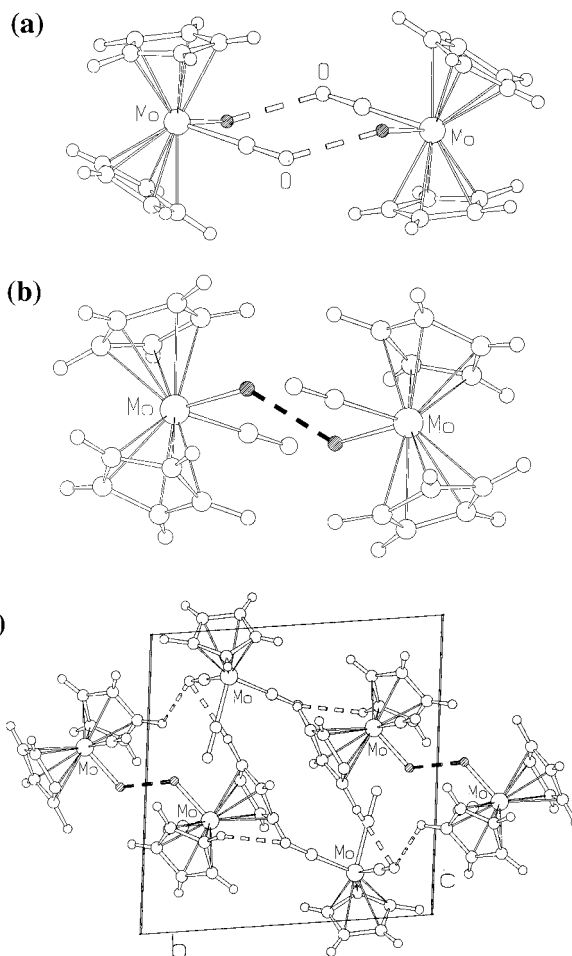


Figure 5. (a) Monoclinic form I of $[(\eta^5\text{-C}_5\text{H}_5)_2\text{MoH}(\text{CO})][(\eta^5\text{-C}_5\text{H}_5)\text{Mo}(\text{CO})_3]$, CPCBMO, showing Mo-H...O intermolecular interactions. (b) Triclinic form II showing different orientations of the cations and longer Mo-H...O distances. (c) The H...H and C-H...O interactions in the triclinic form I.

The compound $[(\eta^5\text{-C}_5\text{H}_5)_2\text{MoH}(\text{CO})][(\eta^5\text{-C}_5\text{H}_5)\text{Mo}(\text{CO})_3]$ ^{17,18} has already been discussed by some of us in a preceding publication.² As mentioned earlier, the compound crystallizes in two different forms. In the monoclinic form I (CPCBMO) the Mo-H...O distances are short, suggesting intermolecular interactions¹⁷ (see Figure 5a), but in the triclinic form II (CPCBMO01) the different orientations of the cations lead to much longer Mo-H...O distances.¹⁸ This change in orientation of pairs of cations in the triclinic form brings the neighboring hydrides together [$\text{H}(1)\cdots\text{H}(1) = 2.234$ Å] (see Figure 5b). It is worth mentioning that, beside the interactions involving the hydride ligands, there are several C-H...O close contacts (>2.4 Å) between cations and anions. The H...H and C-H...O short distances in the triclinic form I are represented in Figure 5c.

The EH calculations were done using the coordinates taken from the experimental structures. An attractive interaction is found in both compounds, as reflected by the positive, though small, overlap populations: CO...H 0.024 and H...H 0.004, respectively, for the two conformers. In the first case, there is an electrostatic interaction between the positively charged hydride (0.164) and the negatively charged oxygen (-0.662), while in the H...H dimer the situation parallels that found for the $\text{HMn}(\text{CO})_5$ dimer.

The zirconocene derivative $[(\eta^5\text{-C}_5\text{H}_5)_2\text{Zr}(\mu\text{-H})(\text{OSO}_2\text{CF}_3)]_2\cdot$

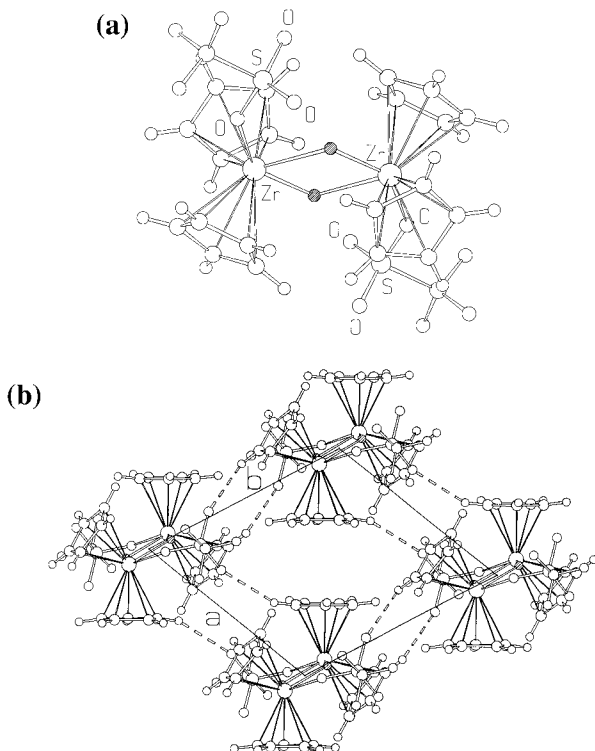
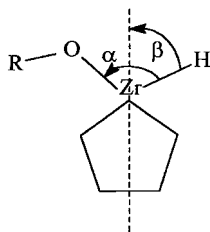


Figure 6. (a) Zirconocene derivative $[(\eta^5\text{-C}_5\text{H}_5)_2\text{Zr}(\mu\text{-H})(\text{OSO}_2\text{CF}_3)]_2 \cdot 0.5\text{THF}$, YUSSOU, forms a dimer via $\text{Zr-H} \cdots \text{Zr}$. (b) $\text{C-H} \cdots \text{O}$ interactions in crystalline $[(\eta^5\text{-C}_5\text{H}_5)_2\text{Zr}(\mu\text{-H})(\text{OSO}_2\text{CF}_3)]_2 \cdot 0.5\text{THF}$.

Chart 3



0.5THF , YUSSOU,²² is observed in the crystal as a dimer, formed by bringing the hydride of one molecule into close contact with the Zr atom of the neighbor molecule (see Figure 6a and Chart 3 below). The vicinity of the bridging hydrides leads to a short $\text{H}(1) \cdots \text{H}(1)$ distance of 2.122 Å. The presence of potential H-bond acceptors in the triflate ligand, (OSO_2CF_3), results in intermolecular interactions of these dimers in the solid state. As shown in Figure 6b, the $\text{C-H} \cdots \text{O}$ interactions arrange four dimers in a tetrameric unit in the ab plane.

$[(\eta^5\text{-C}_5\text{H}_5)_2\text{Zr}(\mu\text{-H})(\text{OSO}_2\text{CF}_3)]_2$ requires a different theoretical approach from the previous ones. If we decompose the dimer into two parts, we obtain a 16-electron Zr(IV) complex with unusual geometry for a bent metallocene derivative. Note that in the previously discussed complex, the cation $[(\eta^5\text{-C}_5\text{H}_5)_2\text{MoH}(\text{CO})]^+$ is an 18-electron species and the type of approach found in the structure of $[(\eta^5\text{-C}_5\text{H}_5)_2\text{Zr}(\mu\text{-H})(\text{OSO}_2\text{CF}_3)]_2$ would have been forbidden. The H-Zr-O angle is extremely large [134.8°], even for d^0 derivatives, where it is expected to be larger than for d^1 and d^2 complexes. An earlier EH study predicted a value of ca. 100° for d^0 Cp_2ML_2 complexes, where $\text{L} = \sigma$ -donor.²³ Experimental angles usually comply with to this rule

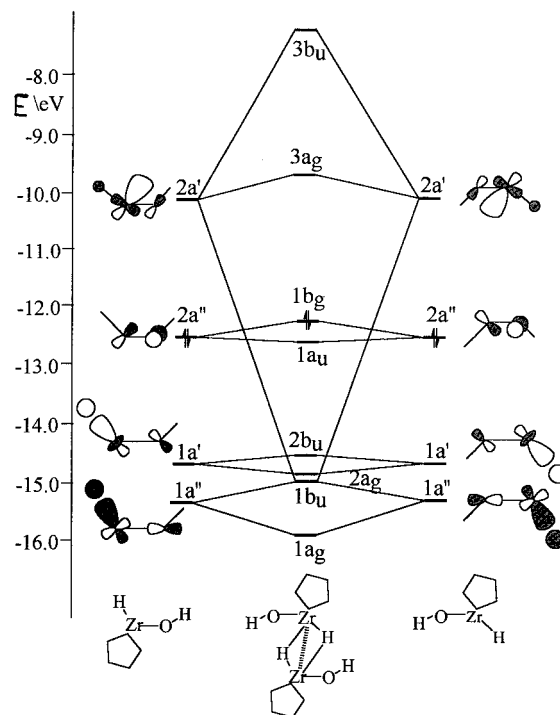


Figure 7. Molecular orbital diagram showing schematically the interaction between two $\text{Cp}_2\text{ZrH}(\text{OH})$ units.

and a search in the Cambridge Structural Database revealed that for the large majority of Cp_2ZrL_2 complexes the L-Zr-L angle falls in the $95\text{--}100^\circ$ range. Exceptions are “false” Cp_2ZrL_2 species, such as YUSSOU. When three ligands beside Cp are present, the angle spanned by the two exterior ones has to be larger. The other feature of crystalline YUSSOU is an asymmetry of ligand distribution in the H-Zr-O plane. Indeed, the plane bisecting the plane defined by Zr and the normals to the two Cp rings does not bisect the H-Zr-O angle (see Chart 3). Such a behavior has been observed in related compounds where two ligands of very different bulkiness coordinate the same metal center, namely, one hydride and another ligand, and has been explained by electronic and steric arguments.²⁴

We started by trying to optimize the angles around Zr in the monomer, by adjusting either α (the H-Zr-O angle) or β , which measures the asymmetry (Chart 3).

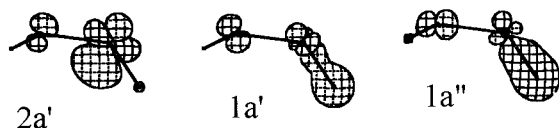
In our zirconocene derivative, the optimum geometry is calculated for $\alpha = 95^\circ$ and $\beta = 54.5^\circ$, the energy being 0.35 eV lower than the experimental one ($\alpha = 135^\circ$ and $\beta = 73^\circ$). This indicates that the molecule in the crystal distorts in order to adapt itself to the arrangement found in the dimer. In the monomer, however, the tendency is to optimize the bonding of the ZrCp_2 fragment with the ligands. Indeed, overlap populations increase when α goes from 135 to 95° (for Zr-O , from 0.40 to 0.42, and for Zr-H , from 0.63 to 0.64, respectively) and the OR ligand occupies a position which allows for π -bonding between the appropriate oxygen lone pair and the $1a_1$ orbital of the zirconocene (see ref 23 and Figure 7 below), which is empty in this d^0 complex. Both the need to maximize π -bonding and the different bulkiness of the ligands account for the detected asymmetry. This latter reflects the repulsion between ligand and Cp hydrogens,²⁴ which is larger for OR than for H. Therefore, the angle between the Zr-O bond and the central line (dashed line in Chart 3), $\alpha - \beta = 62^\circ$, is

(22) Luinstra, G. A.; Rief, U.; Prosenc, M. H. *Organometallics* **1995**, *14*, 1551.

(23) Lauher, J. W.; Hoffmann, R. *J. Am. Chem. Soc.* **1976**, *98*, 1729.

(24) Azevedo, C. G.; Calhorda, M. J.; Carrondo, M. A. A. F. de C. T.; Dias, A. R.; Félix, V.; Romão, C. C. *J. Organomet. Chem.* **1990**, *391*, 345.

Chart 4



narrower than the angle between Zr–H and the same line, $\beta = 73^\circ$. Notice that these calculations were done using R = H as a model for triflate and that the experimental details are well reproduced.

We have therefore concluded that the monomer distorts at the expense of non-negligible energy in order to reach the geometry needed to form the dimer. We are going to see next that in this geometry an extra Zr–H bond may be formed, which makes the overall process energetically favorable. The most relevant interactions between two $\text{Cp}_2\text{ZrH}(\text{OH})$ units are depicted in Figure 7. They can essentially be described as donation from the Zr–H bonding orbital 1a'' in one (the symmetry labels refer to the monomer) to an empty Zr-centered orbital 2a' of the second, the π -antibonding counterpart of the interaction between the O atom p orbital and the zirconocene 1a₁ orbital. A second Zr–H bonding orbital (1a') mixes in, so that the global interaction involves six fragment orbitals. These three orbitals are drawn in a three-dimensional representation in Chart 4.

The HOMO of the dimer is also shown in Figure 7 and results from a four-electron destabilizing interaction between the HOMOs of the two monomers. There is a large HOMO–LUMO gap in the final species.

In view of the character of the orbitals participating in the bonding (Chart 3), it might be assimilated to an agostic interaction, i.e. an M–H ···M agostic bond. Indeed, the Zr–H orbitals (1a', 1a'') donate part of their electrons into the empty Zr orbital 2a'. This observation lends further support to the existence of the so-called intermolecular pseudo-agostic (IPA) interaction between electron-deficient coordinatively unsaturated metal complexes and electron-rich counterions.⁷ Prototypical examples are Marks' electron-deficient zirconocene complexes.²⁵ During this process, besides the new Zr–H bond, a Zr–Zr bond is also formed and the two hydrogen atoms are forced to come into close contact, which explains why this molecule has come into our structural sample (Scheme 1).

The lowest energy MO is both Zr–H and H–H bonding. The second one is Zr–H bonding, but H–H antibonding. Although part of the H–H antibonding character has been relieved by mixing in a bonding way of the empty high-energy orbitals (2a'), such mixing is not enough to overcome its antibonding character and not even a weak H ···H bond remains. The H ···H overlap population is -0.007 . Therefore, the driving force for dimerization is the formation of Zr–H and Zr–Zr covalent bonds. The compound observed in the crystal structure is better described as containing 18-electron Zr complexes with three monodentate ligands, OR and two nonequivalent hydrides, one closer than the other, rather than a dimer of the 16-electron $\text{Cp}_2\text{ZrH}(\text{OH})$ species. In the final species, the overlap populations are Zr–H 0.472 and 0.217, Zr–O 0.392, Zr–Zr 0.145. This situation is therefore totally different from what has been observed before in the complexes referred to above.

Intermolecular Interactions of the M–H ···H–C Type. The complex $\text{mer}[(\text{Me}_3\text{P})_3\text{IrH}(\text{Cl})(\text{C}_5\text{H}_4\text{N})]$, LANMES,²⁶ pre-

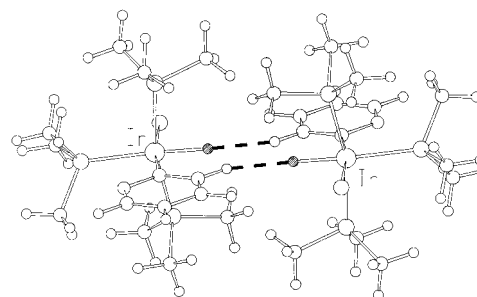
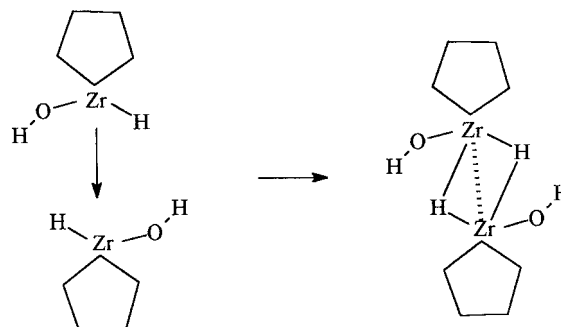


Figure 8. Intermolecular interactions in crystalline $\text{mer}[(\text{Me}_3\text{P})_3\text{IrH}(\text{Cl})(\text{C}_5\text{H}_4\text{N})]$, LANMES.

Scheme 1



sents an iridium octahedrally coordinated to three phosphines, a hydride, a chloro ligand, and finally a 2-pyridyl ligand via its ortho C atom. It is a C–H group of this ring that interacts with the hydride of the adjacent molecule (H ···H distance 2.106 Å) to form a dimer, as depicted in Figure 8.

The solid-state structure of $\text{mer}[(\text{Me}_3\text{P})_3\text{IrH}(\text{Cl})(\text{C}_5\text{H}_4\text{N})]$ represents well the case in which the intermolecular M–H ···H–M short contact discussed in the previous section is replaced by an M–H ···H–C interaction. The C–H donor group may belong either to a cyclopentadienyl ligand, or to an alkyl or aryl in a ligand or to a solvent molecule. M–H ···H–C short contacts are far more frequent than M–H ···H–M ones, these latter interactions requiring close approach of hydrogen atoms most often deeply embedded within the ligand coverage.

In the complex $\text{mer}[(\text{Me}_3\text{P})_3\text{IrH}(\text{Cl})(\text{C}_5\text{H}_4\text{N})]$, LANMES,²⁶ the 2-pyridyl ligand is not coordinated through the nitrogen atom, and this atom is not involved in any intramolecular interaction. Indeed, the N atom is on the side of the molecule opposite the hydride, and it was found that there was no free rotation in solution.

The model used in the calculations was $\text{mer}[(\text{H}_3\text{P})_3\text{IrH}(\text{Cl})(\text{C}_5\text{H}_4\text{N})]$ and the orientation of the pyridyl ring was optimized. The most stable conformation corresponds to the one experimentally observed, with the nitrogen trans to the hydride. A rotation away from this position leads to a high-energy barrier (0.7 eV) with a maximum for 90° (vertical ring) which has clearly a steric origin. Further rotation until 180° leads us to a geometry where the ring is again lying on the equatorial plane with the N atom cis with respect to the hydride. The energy is ca. 0.5 eV higher than for 0° , in agreement with the observed structure (Chart 5).

This same problem was handled by atom–atom potential calculations.²⁷ It was found that the barrier to rotation of the 2-pyridyl ring is very high (ca. 600 kJ mol⁻¹), the maximum corresponding again to the vertical orientation. This barrier can be ascribed partly to intramolecular repulsions (ca. 290 kJ mol⁻¹)

(25) Yang, X.; Xinmin, Y.; Stern, C. L.; Marks, T. J. *J. Am. Chem. Soc.* **1994**, *116*, 10015.

(26) Selnau, H. E.; Merola, J. S. *Organometallics* **1993**, *12*, 1583.

(27) Braga, D. *Chem. Rev.* **1992**, *92*, 633.

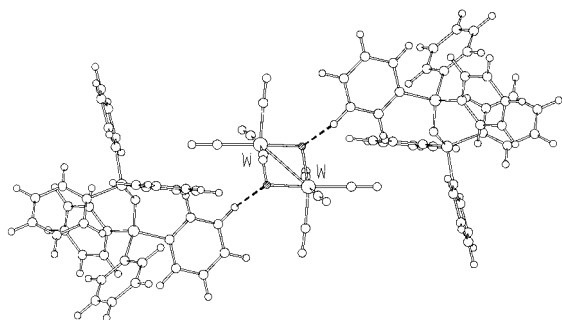
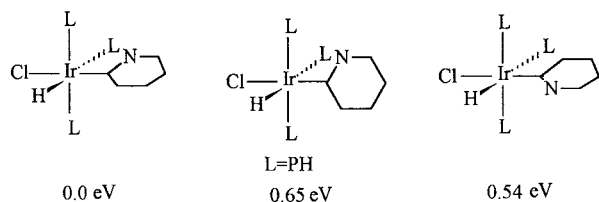


Figure 9. Solid-state molecular structure of ditungsten complex $[(\text{Ph}_3\text{P})_2\text{N}]_2[\text{H}_2\text{W}_2(\text{CO})_8]$, BIKBEC01, showing a distortion of the axial carbonyls

Chart 5



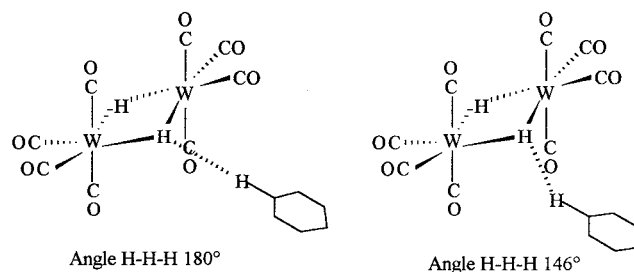
and the remaining to an intermolecular contribution (ca. 310 kJ mol^{-1}), as rotation of the ring also interferes with ligands of the adjacent molecules. The high intramolecular barrier is in agreement with the static behavior in solution.²⁶

In the monomeric Ir complex, the charge distribution is consistent with that expected, namely, negative charges are found for the hydride (-0.08), the chlorine (-0.75), the 2-pyridyl nitrogen (-0.91), while the H(C) which approaches another complex molecule to form the dimer carries a small positive charge of 0.03 . Upon dimer formation, these charges vary only minimally, and we cannot draw conclusions, but their values point toward an electrostatic interaction responsible for dimerization. We cannot find a net stabilization during this process, but the energy changes are not very significant. On the other hand, according to our calculations, the alternative M-H...H-M association pathway is not favored as it was for $\text{HMn}(\text{CO})_5$. Although for an H...H distance of 2.2 \AA the overlap population (0.037) is indicative of attraction, the energy has greatly increased.

The structure of the ditungsten complex $[(\text{Ph}_3\text{P})_2\text{N}]_2[\text{H}_2\text{W}_2(\text{CO})_8]$,²⁸ BIKBEC01, has been determined by both X-ray or neutron diffraction. The authors observed that the structure of the anion in the solid state shows a distortion of the axial carbonyls and that the $[(\text{Ph}_3\text{P})_2\text{N}]^+$ counterion shows an unusual staggered conformation of the phenyl rings. The short H...H contact (2.150 \AA , see Figure 9) links the tungsten dianion to the two cations, a pattern that is seen in other examples. In addition, there is a diffuse network of bifurcated and trifurcated C-H...O interactions in the range $2.477\text{--}2.565 \text{ \AA}$, formed by the phenyl hydrogens.

This compound differs from the one discussed above because the hydride ligand interacting with the H(C) system is a bridging hydride. In a previous work involving other polynuclear hydride species,² we found that bridging hydrides tend to exhibit an acidic character with the hydrogen atom carrying a small positive charge that allows formation of M-H...O interactions. The apparent anomaly showed by the binuclear dianion $[\text{W}_2(\mu\text{-H})_2(\text{CO})_8]^{2-}$ ²⁸ called for an investigation.

Chart 6



In the model structure, the W_2H_2 atoms were taken to be coplanar, but the small distortion of the axial carbonyl groups away from the vertical was ignored. In this dianion, we find that the hydrides carry a negative charge irrespective of the parameters used (see Experimental Section), although the charges are different. The change of parameters only significantly affects the charge distribution between the metal (0.032 for normal hydride parameters, -0.164 for modified) and the hydride (-0.374 , -0.114 , respectively), leaving the carbonyls almost unchanged. As the nature of the interaction between the dianion and the H(C) in the neighbor group stays qualitatively the same, the following results refer to the calculation with modified hydride parameters, for the sake of comparison. In the crystal structure, the organometallic dianion exhibits short contacts between each of the two hydrides and two H(C) atoms of the phenyl groups in the two counterions (see Figure 9), reflecting the presence of an inversion center at the middle of the W_2H_2 rhombus. For simplicity, we only allowed one benzene to approach one side of the dianion, to estimate the nature of the possible interaction taking place. Again, the potential energy surface for approaching the phenyl group is very soft, though slightly repulsive. At the experimental H...H distance of 2.15 \AA , the H...H overlap population has increased up to 0.007 , while the negative charge on the hydride (-0.114) and the positive charge on the H(C) atom (0.033) are compatible with an electrostatic origin of the interaction. This explanation should hold more strongly in the real structure, where the group approaching the dianion is not a neutral benzene but a phenyl substituent of a positively charged cation. Therefore, the driving force for bringing anion and the cations together is chiefly of electrostatic nature. What we can probe, namely charge distribution and overlap populations, fits well in the picture. We also tried several approaches of the phenyl group: along the W_2H_2 plane (Chart 6, left) or with a geometry similar to that found (Chart 6, right). The second approach is more repulsive, and at least part of the extra repulsion can be traced to the ring getting close to the two axial carbonyls.

As a matter of fact, the same approach with a vertical benzene ring is less repulsive. Another way to relieve pressure, at least partially, would be to force the axial carbonyls to move away from their vertical position, in a distortion very similar to what is found in the structure. Of course, in the real structure, the same is happening on both sides of the molecule, so that all axial carbonyl groups become distorted.

The complex $(\eta^5\text{-C}_5\text{H}_5)_2\text{TaH}(\text{CO})$,²⁹ BISZIM, shows a remarkably short H...H intermolecular interaction of 1.957 \AA between the tantalum-coordinated hydride ligand and a Cp hydrogen atom. The H...H overlap population calculated using the coordinates of the real structure is 0.011 . In addition to the unique carbonyl group participates in a total of four

(28) Wei, C.-Y.; Marks, M. W.; Bau, R.; Kirtley, S. W.; Bisson, D. E.; Henderson, M. E.; Koetzle, T. F. *Inorg. Chem.* **1982**, *21*, 2556.

(29) Gagliardi, J. A.; Teller, R. G.; Vella, P. A.; Williams, J. M. *Cryst. Struct. Commun.* **1982**, *11*, 861.

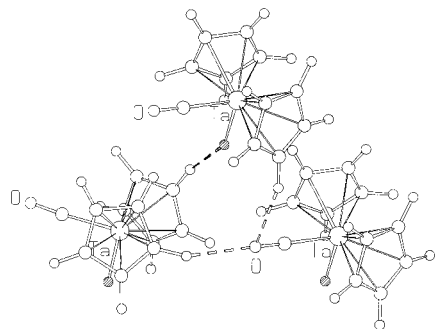


Figure 10. Ta–H ··· H–C and two of the four C–H ··· O–C interactions in crystalline $(\eta^5\text{-C}_5\text{H}_5)_2\text{TaH}(\text{CO})_2$, BISZIM.

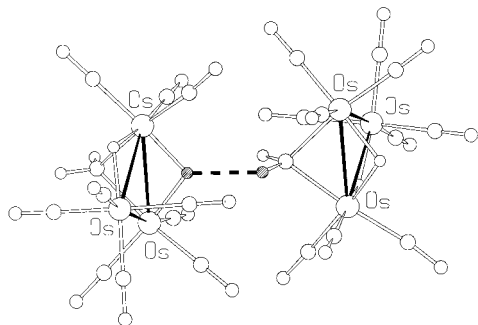


Figure 11. H ··· H interaction [H(1) ··· H(4) 2.085 Å] between one CH_2 hydrogen and one of the bridging hydrides in crystalline $\text{Os}_3(\mu_2\text{-H})_2(\mu_3\text{-CH}_2)(\text{CO})_{10}$, DCHMOS01.

C–H ··· O bonds (see Table 1) probably because of the absence of competing acceptors. The most important interactions are shown in Figure 10.

The complex $\text{Os}_3(\mu_2\text{-H})_2(\mu_3\text{-CH}_2)(\text{CO})_{10}$, DCHMOS01,³⁰ carries a methylene ligand and two bridging hydrides. The crystal shows the presence of an H ··· H interaction [H(1) ··· H(4) 2.085 Å], between one CH_2 hydrogen and one of the bridging hydrides, as shown in Figure 11. The H ··· H overlap population is 0.005, both hydrogen atoms having a positive charge. This is observed for many bridging hydrides. As a result, this interaction is more similar in nature to that observed in $\text{HMn}(\text{CO})_5$ than those found in M–H ··· H–C situations.

The two hydride complexes of rhenium $\text{ReH}(\text{CO})_2(\text{PMe}_3)_3$ (HAKCUR) and $\text{ReH}_5(\text{CO})(\text{PMe}_3)_3$ (HAKDEC)³¹ show the presence of very short H ··· H intermolecular distances between one hydride and a methyl hydrogen (1.839 Å for HAKCUR and 1.890 Å for HAKDEC). The H ··· H overlap population is 0.023 and 0.017, respectively. These interactions link molecules in pairs in the solid state. In addition to Re–H ··· H–C interactions, C–H ··· O hydrogen bonds are present in both crystals (see Table 1). Figure 12 shows the principal interactions in the case of HAKCUR.

The platinum salt $\text{trans-}[\text{PtH}(\text{PhHNNC}_3\text{H}_6)(\text{PPh}_3)_2][\text{BF}_4]$, HAPZPT10,³² crystallizes together with a benzene molecule (Pt–H ··· H–C distance 2.092 Å) as shown in Figure 13. The H ··· H overlap population is extremely small (0.008, calculated using the cation and the solvent molecule). H ··· F intermolecular distances range from 2.043 to 2.550 Å, the shortest one being an N–H ··· F hydrogen bond involving the hydrazone nitrogen.

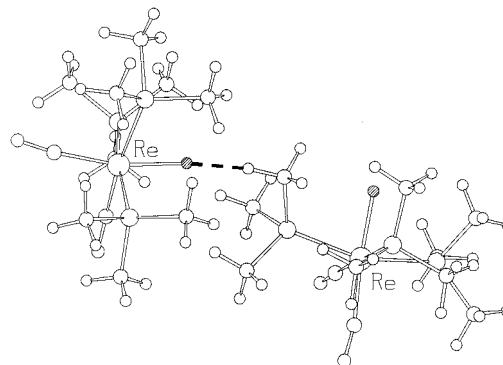


Figure 12. Re–H ··· H–C interaction in crystalline $\text{ReH}(\text{CO})_2(\text{PMe}_3)_3$, HAKCUR.

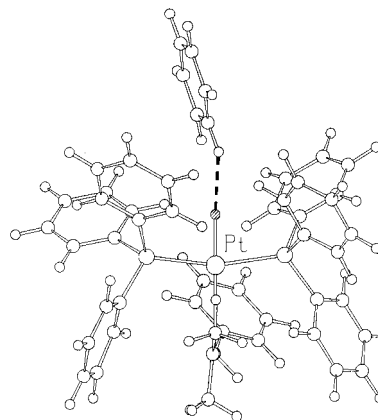


Figure 13. Pt–H ··· H–C interaction between the solvate benzene molecule and the complex $\text{trans-}[\text{PtH}(\text{PhHNNC}_3\text{H}_6)(\text{PPh}_3)_2]^+$, HAPZPT10.

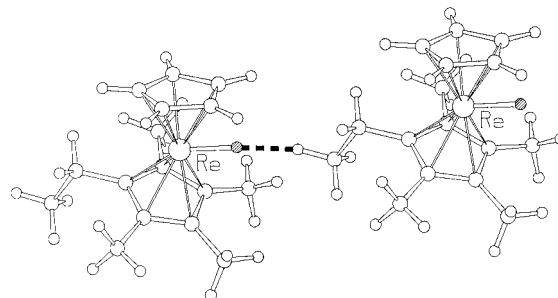


Figure 14. Re–H ··· H–C interactions in crystalline $(\eta^5\text{-C}_5\text{Me}_4\text{Et})(\eta^5\text{-C}_5\text{H}_5)\text{ReH}$, JASRAW.

A short intermolecular M–H ··· H–C distance is also observed in crystalline $(\eta^5\text{-C}_5\text{Me}_4\text{Et})(\eta^5\text{-C}_5\text{H}_5)\text{ReH}$, JASRAW,³³ where the Re–H ··· H–C contact (1.773 Å) involves a hydrogen atom belonging to the ethyl substituent of the cyclopentadienyl ring which forms chains of molecules along the *c* axis, as shown in Figure 14. The H ··· H overlap population, calculated for a dimer of molecules, is 0.016.

In the thioether-coordinated ruthenium complex, $\text{trans-RuH}(\text{Cl})\text{L}$ [where L = *syn*-Me₄[14]aneS₄], KEGCEE,³⁴ there are two main interactions, a Ru–H ··· H–C interaction of 2.009 Å, and a short C–H ··· Cl hydrogen bond (H ··· Cl 2.629 Å, see Figure 15). The calculated H ··· H overlap population in this compound is 0.008, the hydride exhibiting a charge of –0.110 and the other hydrogen involved exhibiting a positive charge of 0.022.

(30) Schultz, A. J.; Williams, J. M.; Calvert, R. B.; Shapley, J. R.; Stucky, G. D. *Inorg. Chem.* **1979**, *18*, 319.

(31) Gusev, D. G.; Nietlispach, D.; Eremenko, I. L.; Berke, H. *Inorg. Chem.* **1993**, *32*, 3628.

(32) Krogsrud, S.; Toniolo, L.; Croatto, U.; Ibers, J. A. *J. Am. Chem. Soc.* **1977**, *99*, 5277.

(33) Paciello, R. A.; Kiprof, P.; Herdtweck, E.; Herrmann, W. A. *Inorg. Chem.* **1989**, *28*, 2890.

(34) Yoshida, T.; Adachi, T.; Ueda, T.; Tanaka, T.; Goto, F. *J. Chem. Soc., Chem. Commun.* **1990**, 342.

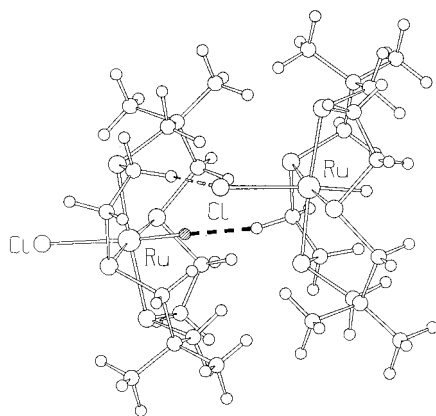


Figure 15. Chains of molecules of *trans*-[RuH(Cl)(*syn*-Me₄[14]aneS₄)], KEGCEE, showing the Ru–H...H–C and the C–H...Cl short contacts responsible for their formation.

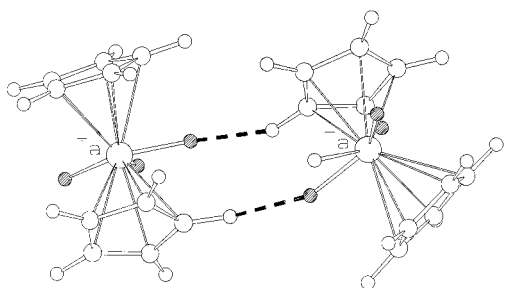


Figure 16. Intermolecular Ta–H...H–C interactions forming centrosymmetric molecular “dimers” in crystalline (η^5 -C₅H₅)₂TaH₃, TACPTH.

The molecular and crystal structures of the tantalum complex (η^5 -C₅H₅)₂TaH₃, TACPTH,³⁵ have been structurally determined by both X-ray and neutron diffraction at 90 K. This latter determination allows a confident description of the two Ta–H...H–C contacts involving the cyclopentadienyl hydrogens (2.002 and 2.093 Å) which form centrosymmetric “dimers” as shown in Figure 16. Both correspond to slightly bonding interactions, the overlap populations being 0.011 and 0.008, respectively.

A similar pattern is shown (Figure 17) by the crystalline polyhydride osmium derivatives H₄Os(PPhMe₂)₃, THMPOS01.³⁶ Os–H...H–C(phenyl) distances of 2.062 Å separate the two molecules within the centrosymmetric “dimer”.

A short Os–H...H–C distance of 2.009 Å is present also in the crystal structure of [H₅Os(PPhMe₂)₃][BF₄], YELZOE,³⁷ which is very much related to that of THMPOS01. The main difference at the intermolecular level is that in the neutral Os compound no other close contacts are seen, while in YELZOE the presence of the counterion leads to several C–H...F intermolecular bonds ranging from 2.225 to 2.507 Å. The size of the dimers prevented us from carrying out the calculations in the real structure, but there is no reason to expect a different result from all previous ones.

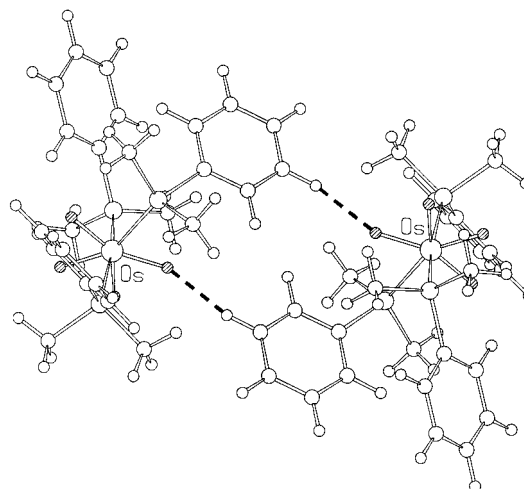


Figure 17. Intermolecular Os–H...H–C interactions forming centrosymmetric molecular “dimers” in crystalline H₄Os(PPhMe₂)₃, THMPOS01.

Conclusions

The great interest in noncovalent bonds accompanying the boom of supramolecular chemistry studies³⁸ has led to a systematic investigation of extramolecular interactions between molecules and ions. It is quite natural that the wealth of structural information on tens of thousand of molecular crystals deposited in the Cambridge Structural Database could become a source of new discoveries on interactions between atoms and molecules.

A molecular crystal has been well described as a giant supermolecule whose chemical and physical properties depend on the complex interplay between molecular features and intermolecular interactions.³⁹ This interplay becomes more complex and intriguing in organometallic crystals because of the combination of “organic type” extramolecular interactions due to the ligands (usually organic molecules or molecular fragments) with the presence of metal atoms and their specific electronic and steric requirements. On this premise, it is thus not surprising that an investigation of extramolecular interactions in organometallic crystals is bringing to light the direct (or indirect) participation of the metal atoms as a key feature, whose importance in supramolecular chemistry as a whole cannot be underestimated.

M–H...X, X–H...M, and M–H...H–X where M is a transition metal and X a main group electronegative atom are “new” bonds which, though weak, may play a crucial role in *fine-tuning* chemical reactivity at the metal centers. The understanding of these “new” bonds requires the use of complementary tools. We have found that one way to proceed is that of “mining” the CSD compounds conforming to some predefined selection criteria (usually a crude distance cutoff), followed by an analysis of the distribution and geometry of extramolecular interactions and the simultaneous investigation of the bonding features both at intra- and intermolecular levels by EH molecular orbital and DFT calculations. These methods, if applied together, can give a more comprehensive picture of the importance and occurrence of weak interactions.

(35) Wilson, R. D.; Koetzle, T. F.; Hart, D. W.; Kwick, A.; Tipton, D. L.; Bau, R. *J. Am. Chem. Soc.* **1977**, *99*, 1775.

(36) Hart, D. W.; Bau, R.; Koetzle, T. F. *J. Am. Chem. Soc.* **1977**, *99*, 7557.

(37) Johnson, T. J.; Albinati, A.; Koetzle, T. F.; Ricci, J.; Eisenstein, O.; Huffman, J. C.; Caulton, K. G. *Inorg. Chem.* **1994**, *33*, 4966.

(38) Lehn, J. M. *Angew. Chem., Int. Ed. Engl.* **1990**, *29*, 1304.

(39) Dunitz, J. D. In *Perspectives in Supramolecular Chemistry. The Crystal as a Supramolecular Entity*; Desiraju, G. R., Ed.; John Wiley & Sons: Chichester, 1996.

In this paper we have analyzed extramolecular interactions of the M–H–H–M and M–H–H–C type. Interestingly, interactions of this type have been known for a long time, the first observations of unusual behaviors dating back not less than thirty years. Most of these observations were made in the course of solid state studies. The overall frame of analysis was, however, obscure and these observations remained unexplained. We are now able to demonstrate that weak attractive interactions can be established between hydrogen atoms bound to transition metals provided that the approach between molecules is not sterically hindered.

From our calculations we found that M–H–H–M are attractive when the metal atoms are not directly involved. This is seen for the dimers of HMn(CO)₅, where evidence for a H–H weakly bonding interaction has been gathered by utilizing different methods, and for the cationic complex [(η⁵-C₅H₅)₂MoH(CO)]⁺. The third crystal exhibiting a short H–H distance is [(η⁵-C₅H₅)₂Zr(μ-H)(OSO₂CF₃)₂]. In this compound, the dimerization is driven by the formation of the Zr–H bond, the resulting H–H interaction being repulsive.

The other group of compounds was studied in detail for two prototypes, namely *mer*-[(Me₃P)₃IrH(Cl)(C₅H₄N)] and [(Ph₃P)₂N]₂[H₂W₂(CO)₈]. The compounds carry terminal and bridging hydride ligands, respectively. In the latter dianionic carbonyl complex the bridging hydride carries a relatively large negative charge so that the two compounds are similar in behavior, the interaction being between a negatively charged hydride and a positively charged proton. The overlap populations are small as expected from such weak interactions but they are consistently positive. The nature of the M–H–H–M or M–H–H–C interactions present in all other crystalline compounds retrieved from the CSD has been screened by theoretical calculations on the observed molecular structures with coherent results.

Altogether, this study adds new evidence for the amphoteric behavior of the M–H bond, a soft bonding system which can be “tuned” by the other ligands bound to the metal center, by the presence of metal–metal bonds in polynuclear complexes, as well as by the proximity of suitable donors or acceptors. With this work we have seen two manifestations of this behavior: the M–H–H–M bonding can be regarded as the *supra-molecular equivalent* of the covalent bond, whereas the M–H–H–C bonds are the equivalent of a polarized bond between atoms of different electronegativity.

Experimental Section

Cambridge Structural Database (CSD) Analysis. Data were retrieved from the October 1996 version of the CSD for all crystal structures with an exact match between chemical and crystallographic connectivity. Only entries with H–H distances between 1.5 and 2.6 Å were considered. Unique contacts were considered up to an H–H distance of 2.2 Å (van der Waals sum). M–H bond lengths were taken as such and not normalized. Geometrical questions are given in the Supporting Information as representative examples. All the examples were taken from the search outputs and were investigated by computer graphics.^{40a} The computer program PLATON^{40b} was used to analyze the metrical features of the hydrogen bonding patterns.

Molecular Orbital Calculations. Extended Hückel Calculations. The extended Hückel method with modified H_{ij}^s⁴¹ was used. The basis set for the metal atom consisted of *ns*, *np*, and (*n* – 1)*d* orbitals. Only

3s and 3p orbitals were considered for phosphorus and chlorine. The s and p orbitals were described by single Slater-type wave functions, and the d orbitals were taken as contracted linear combinations of two Slater-type wave functions. Standard parameters were used for H, C, O, N, Cl, S, and P, while those for the metals were the following: **Mn** (H_{ij}/eV, ζ) 4s, –9.75, 1.900; 4p, –5.89, 1.900; 3d, –11.67, 5.150, 1.900 (ζ₂), 0.5320 (C₁), 0.6490 (C₂); **W** (H_{ij}/eV, ζ) 6s, –8.26, 2.341; 6p, –5.17, 2.309; 5d, –10.37, 4.982, 2.068 (ζ₂), 0.6940 (C₁), 0.5631 (C₂); **Ir** (H_{ij}/eV, ζ) 6s, –11.30, 2.504; 6p, –4.50, 2.200; 5d, –12.10, 5.796, 2.575 (ζ₂), 0.6353 (C₁), 0.5553 (C₂); **Zr** (H_{ij}/eV, ζ) 5s, –9.870, 1.817; 5p, –6.76, 1.776; 4d, –11.18, 3.835, 1.505 (ζ₂), 0.6211 (C₁), 0.5796 (C₂); **Rh** (H_{ij}/eV, ζ) 5s, –8.090, 2.135; 5p, –4.57, 2.100; 4d, –12.50, 5.542, 2.398 (ζ₂), 0.5563 (C₁), 0.6119 (C₂). Parameters for Mo, Ta, Os, Re, and Pt are those included in the program CACAO.⁴² A set of modified parameters was used for the hydride ligands, according to the procedure of Eisenstein et al.,⁴³ as it gives a better reproduction of their behavior: H (H_{ij}/eV, ζ) 1s, –11.60, 1.000. As stated by these authors, the use of these parameters does not change the nature of the results, it only enhances the hydride behavior. Three-dimensional representations of orbitals and calculations using the observed structures were done using the program CACAO.

Idealized models were used for the complexes studied in more detail, based on their experimentally determined structure. For FOKCEN02, distances were Mn–C 1.85, C–O 1.13, Mn–H 1.6 Å, H–H varied as described in the text, and angles (deg) C_{eq}–Mn–H 85, C_{ax}–Mn–H 180. For YUSSOU, the distances (Å) were Zr–H 1.831, Zr–O 2.20, O–H 1.00, Zr–Cp 2.198, C–C 1.40, and C–H 1.08, and the angles (deg) were H–Zr–O 134.8, Zr–O–H 139.6, Cp–Zr–Cp 127.8, or as described in the text. For BIKBEC01, the distances (Å) were W–H 1.920, W–W 3.010, W–C 2.0, C–O 1.13, C–H 1.08, C–C 1.40, and the angles (deg) C–W–C 90, H–W–H 77. Calculations were performed for the other complexes using the experimentally determined structure, to search for the H–H overlap population or in the previous ones to test the reliability of the models.

Molecular Orbital Calculations. DFT Calculations. The density functional calculations⁴⁴ were carried out on a model for the dimer of HMn(CO)₅ using the Amsterdam Density Functional (ADF) program¹² developed by Baerends and co-workers⁴⁵ using nonlocal exchange and correlation corrections.⁴⁶ The geometry optimization procedure was based on the method developed by Versluis and Ziegler.⁴⁷ The atom electronic configurations were described by a double-ζ Slater-type orbital (STO) basis set augmented with a single-ζ polarization function for C 2s, 2p and O 2s, 2p; a triple-ζ STO augmented with a single-ζ polarization function was used for H 1s; and triple-ζ STO basis set was used for Mn 4s and 4p. A frozen-core approximation was used to treat the core electrons of C, O, and Mn.

The geometry of the monomer was optimized to test the conditions of the calculations, allowing the Mn–H distance and the C_{eq}–Mn–H angle to vary under C_{4v} symmetry. Two monomeric units were allowed to form the dimer starting from the experimental H–H distance, and the approaching geometry was optimized (H–H distance and the angle between the two Mn–H bonds) for both the eclipsed and the staggered geometries under C_s and no symmetry restrictions, respectively.

Acknowledgment. Financial support from the University of Bologna–Project Intelligent Molecules and Molecular Aggregates and the Ministero dell’Università e della Ricerca

(40) (a) Keller, E. *SCHAKAL Graphical Representation of Molecular Models*; University of Freiburg: Freiburg, Germany, 1992. (b) Spek, A. L. *Acta Crystallogr.* **1990**, A46, C31.
(41) Ammeter, J. H.; Bürgi, H.-B.; Thibault, J. C.; Hoffmann, R. *J. Am. Chem. Soc.* **1978**, 100, 3686.

(42) Mealli, C.; Proserpio, D. M. *J. Chem. Educ.* **1990**, 67, 39.
(43) Jackson, S. A.; Eisenstein, O. *J. Am. Chem. Soc.* **1990**, 112, 7203.
(44) Parr, R. G.; Yang, W. *Density Functional Theory of Atoms and Molecules*; Oxford University Press: New York, 1989.
(45) (a) Baerends, E. J.; Ellis, D.; Ros, P. *Chem. Phys.* **1973**, 2, 41. (b) Baerends, E. J.; Ros, P. *Int. J. Quantum Chem.* **1978**, S12, 169. (c) Boerrigter, P. M.; te Velde, G.; Baerends, E. J. *Int. J. Quantum Chem.* **1988**, 33, 87. (d) te Velde, G.; Baerends, E. J. *J. Comput. Phys.* **1992**, 99, 84.
(46) (a) Becke, A. D. *J. Chem. Phys.* **1987**, 88, 1053; **1986**, 84, 4524. (b) Vosko, S. H.; Wilk, L.; Nusair, M. *Can. J. Phys.* **1980**, 58, 1200. (c) Perdew, J. P. *Phys. Rev.* **1986**, B33, 8822. (d) Perdew, J. P. *Phys. Rev.* **1986**, B34, 7406.
(47) (a) Versluis, L.; Ziegler, T. *J. Chem. Phys.* **1988**, 88, 322. (b) Fan, L.; Ziegler, T. *J. Chem. Phys.* **1991**, 95, 7401.

Scientifica e Tecnologica is acknowledged (D.B. and F.G.). We acknowledge CNR (Italy) and JNICT (Portugal) for a joint financial support and the ERASMUS program "Crystallography" (P.D.L.). M.J.C. thanks the HCM European network Quantum Chemistry of Transition Metals Compounds.

Supporting Information Available: Geometrical questions for the search of M–H---H–C intermolecular contacts (1 page). Ordering information is given on any current masthead page.

IC9710014